UWB Monopole Antenna with Switchable Band-Notch Characteristic Using a Novel MEMS Afloat

Arash Nemati and Bahram A. Ganji

Department of Electrical & Computer Engineering
Babol Noshirvani University of Technology, Babol, Mazandaran, Iran
Arash.nemati@stu.nit.ac.ir, baganji@nit.ac.ir

Abstract ─ In this paper, a novel microelectro-mechanical system (MEMS) U-shaped afloat is designed and used instead of a simple slot to activate and deactivate the band notch characteristic of an ultra wideband (UWB) monopole antenna at the WLAN band (5.15-5.825 GHz) without extra DC bias lines. The novelty of this work is design of MEMS afloat that can stay in down state permanently. When the dc actuation voltage, about 20 volts, is applied to the microstrip center line, the $\lambda/2$ long U-shaped afloat moves down and creates a slot (resonating element) in its vacant place. Whereas no voltage is applied, the afloat remains in the up position and serves as a part of the antenna, which eliminates the resonance. The proposed design for MEMS afloat has least negative effect on gain, reflection coefficient, and pattern of the antenna. The gain of the antenna is about 3.2 dBi over the entire UWB frequency band (3.1-10.6 GHz), while it decreases sharply over 7 dB at the rejection band. More-over, the time-domain characteristics of the antenna is investigated, which shows 1 ns delay over the UWB frequency band for 20 cm. Due to a novel afloat design, the addition of the resonance element does not affect on the radiation performance, reflection coefficient, gain, and group delay of the antenna outside of notched band frequencies.

Index Terms ─ MEMS U-shaped afloat, switchable band notch, UWB antenna.

I. INTRODUCTION

In recent years, due to the attractive features, such as low cost, small size, ease of fabrication, and wide frequency bandwidth, there has been more attention in ultrawideband (UWB) monopole antennas. The Federal Communication Commission (FCC) has allocated 3.1-10.6 GHz for commercial ultrawideband (UWB) communication systems [1]. Several antenna structures have been proposed for UWB applications [2-5]. The frequency range for UWB system will cause interference to some other existing narrowband services. One of them is wireless local-area network (WLAN), which operates in the 5.15-5.875 GHz band. However, using filters the

complexity of the UWB system will increase. To over-come this problem, the structures with band-rejection characteristic such as parasitic inverted-U strip [6], U-shaped slot [7-9], arc-shaped slot [10], H-shaped conductor backed plane [11], and rectangle-shaped plane [12] are proposed to integrate with the previous antennas. However, none of them had reconfigurable band notch characteristics. The main challenge for researchers in UWB antenna design is the design of a single antenna that can provide reconfigurable rejected band. Reconfigurability is obtained by employing two ideal switches on SIS-HSIR and SIS-SIR [13]. A pin diode is used in [14] to switch ON or OFF the notch band. However, the switches were actuated using DC bias lines. MEMS switches are used in [15] to reach the reconfigurability without bias lines. However, to reach this capability, a floating ground was used in MEMS switch. Therefore, the switch could not stay in down position permanently.

In this paper, an UWB monopole antenna with U-shaped MEMS afloat that can be actuated to place a band notch at the WLAN frequencies is presented. The MEMS afloat is designed so that it does not require extra bias lines and the switch can stay in down position permanently.

II. DESIGN OF ANTENNA AND MEMS AFLOAT

Figure 1 shows the geometry of the reconfigurable WLAN band rejection UWB elliptical monopole antenna. The antenna was designed on a 28 mm × 37 mm liquid crystal polymer (LCP) substrate with a low permittivity ($\varepsilon r \approx 3$), low-loss ($tan\ \delta \approx 0.002$), and a thickness of 0.3 mm. All of these characteristics make it an ideal substrate for antennas, particularly at high frequencies. The width of the 50 ohm microstrip feed line is 0.75 mm and the thickness of the antenna and the ground plane is 5 μm. In this paper, a novel MEMS afloat is designed and used instead of a simple slot in the antenna. The afloat is held by several beams, which are connected to the antenna in 10 points, shown with red points [Fig. 1 (c)]. The dimensions of the antenna, afloat, beams, bridges,

and ground plane are summarized in Table 1.

The lengths of the beams are:

$$L_{b1} + L_{b2}/2, \quad (1)$$

$$L_{b1} + L_{b3}/2, \quad (2)$$

$$L_{b1} + L_{b4}/2. \quad (3)$$

There is an air gap between afloat and ground plane with depth of h=45 μm.
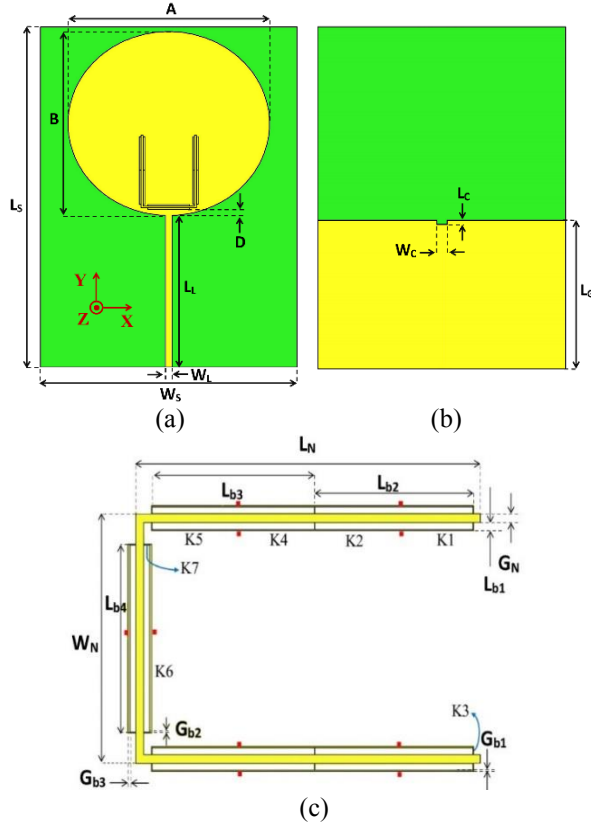

(a)   (b)

(c)

Fig. 1. Schematic diagram of: (a) antenna's front view, (b) antenna's back view, and (c) U-shaped afloat.

Table 1: Antenna and afloat dimensions

Parameter	Length (mm)	Parameter	Length (mm)
L_S	37.000	L_N	7.900
W_S	28.000	G_N	0.200
A	22.000	W_N	6.045
B	20.000	L_{b1}	0.190
L_L	16.500	L_{b2}	3.640
D	0.820	L_{b3}	3.740
L_G	16.400	L_{b4}	4.540
W_L	0.750	G_{b1}	0.030
L_C	0.300	G_{b2}	0.010
W_C	1.000	G_{b3}	0.045

A 1 μm thick high resistive sheet, underneath a passivation layer is at the bottom of air gap, which is

connected to the ground plane. When the dc actuation voltage is applied to the microstrip center line, the $\lambda/2$ long U-shaped afloat moves down (h=45 μm) and creates a slot (resonating element) in its vacant place [Fig. 2 (b)]. Whereas no voltage is applied, the afloat remains in the up position and serves as a part of the antenna, which eliminates the resonance [Fig. 2 (a)].

The pull-in voltage V_{PI} can be expressed as [16]:

$$V_{PI} = \sqrt{\frac{8 K h^3}{27 \varepsilon_0 A}}, \quad (4)$$

where h is the original gap between afloat and ground plane, ε_0 is the dielectric constant of the air, A is the surface area of the afloat, which for the afloat design can be expressed as:

$$A = \left(2\left(G_N \times L_N\right) + \left(G_N \times W_N\right)\right), \quad (5)$$

and K is the effective spring constant of the 20 T-shaped and L-shaped beams [Fig. 1 (c)], which can be written as:

$$K = 4\left[\begin{array}{c}\left(K_1 \| K_3\right) + \left(K_2 + K_4\right)\| K_3 + \\ +\left(K_5 \| K_3\right) + \left(K_6 \| K_7\right)\end{array}\right], \quad (6)$$

where:

$$K_i = \frac{E G_i T_i^3}{L_i^3}, \quad (i=1,2,...,7) \quad (7)$$

where L_i, G_i, and T_i are the length, width, and thickness of the beams, and E is the Young's modulus of the aluminum. Firstly, the values of Table 1 should be put in Eq. 7 to calculate the K_i for all of the beams. Secondly, the results from Eq. 7 should be put in Eq. 6 to calculate the effective spring constant of the afloat.
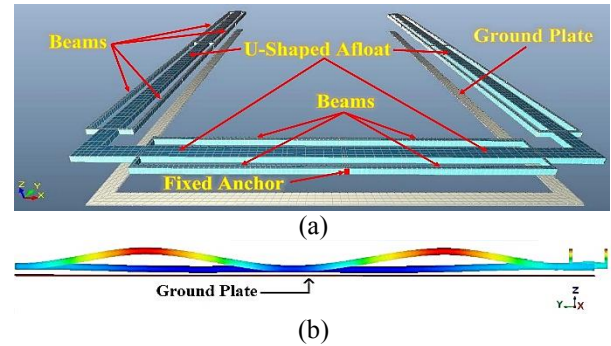

(a)

(b)

Fig. 2. Schematic diagram of U-shaped MEMS afloat and ground plate in: (a) up position and (b) down position.

The radiating structure, located at a distance 0.1 mm from the end of the ground plane, is an elliptical antenna, which has a major axis A=22 mm and a secondary axis B=20 mm. Depending on the lowest frequency of operation (f_l=3.1 GHz) and effective dielectric constant of substrate, A and B are calculated as:

$$\frac{1}{2}\left(\pi \cdot \frac{(A+B)}{2}\right) + L_L = c\Big/\left(2 f_\ell \sqrt{\varepsilon_{eff}}\right), \quad (8)$$

where:

$$\varepsilon_{eff} = (\varepsilon_r + 1)/2, \qquad (9)$$

where c is the speed of light. The left side of the Eq. 8 is the half of the circumference of the antenna and its transmission line. The antenna and its transmission line together act as a monopole antenna. Hence, their total length should be equal to half of the frequency which the antenna is supposed to radiate. Since the UWB antenna radiates at very large range of frequency, the lowest frequency determines the total size of the antenna. Next, attenuation would happen at twofold the lowest frequency and the next one at threefold that frequency. As a result, A and B are chosen and then according to Eq. 8, L_L is calculated. Figure 3 shows optimization of parameters A and B to achieve best result for the reflection coefficient of the antenna. The best values for A and B is selected to have the lowest S_{11} over the entire UWB frequency band (3.1-10.6 GHz).

Additionally, the antenna performance in the high frequency band (between 9 GHz to 11 GHz) can be further improved by cutting a rectangular slot on the middle of the ground plane. Figure 4 shows the optimization of parameter L_C to achieve best result for the reflection coefficient of the antenna. $L_C = 0.3$ mm is selected to decrease the reflection coefficient and also does not affect other frequency ranges so much.
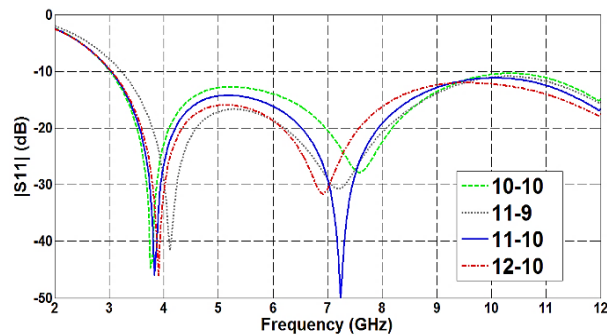

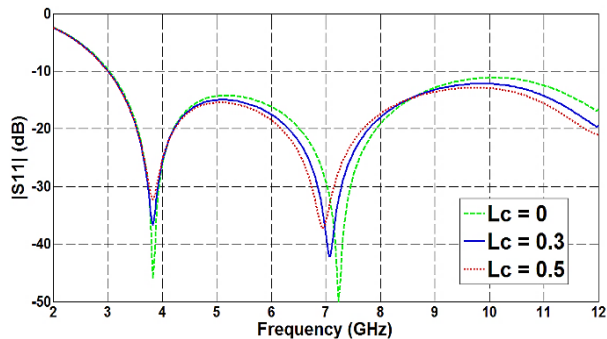Fig. 3. Effect of antenna size on reflection coefficient (A/2 – B/2).

Fig. 4. Effect of L_C on reflection coefficient.

III. OPERATION PRINCIPLE

The total length of the slot is approximately $\lambda/2$ at the frequency which the rejection band is desired (around 5.5 GHz). The relation between central notched frequency and afloat dimensions can be approximately considered as [17]:

$$f_U = c/\left(4\left(L_N + (W_N/2) - G_N\right)\sqrt{\varepsilon_{eff}}\right), \qquad (10)$$

where L_N, W_N, and G_N are the length, width, and thickness of the afloat, and ε_{eff} is the effective dielectric constant of the air.

Figure 5 shows the surface current distribution in two frequencies. As shown in Fig. 5 (a), at the notch frequency of 5.5 GHz, when the afloat is in down position the current density in the edges of the U-shaped slot is stronger than other areas. The directions of the currents in the inner and outer side of the U-shaped slot are opposite to each other as presented in [16]. Therefore, they cancel each other and the antenna does not radiate. On the other hand, in Fig. 5 (b), we can see stronger current distributions concentrated near the outer edges of the antenna at the center frequency of the corresponding notched band. At a pass band frequency of 8 GHz (outside the notched band), the distribution of the surface current is uniform near the outer edges of the antenna, as shown in Fig. 5 (c).
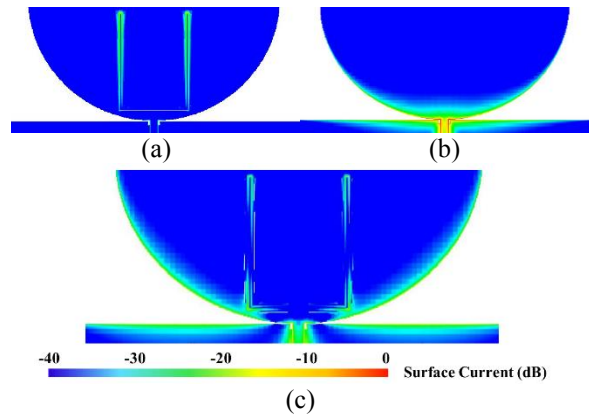

Fig. 5. Simulated surface current distributions: (a) afloat down at 5.5 GHz, (b) afloat up at 5.5 GHz, and (c) afloat down at 8 GHz.

The slot can be modeled by a short circuit terminated series stub in a transmission line model as shown in Fig. 6. The presence of the slot is modeled as a long, short circuit terminated series stub, which is similar to a spur line filter. If the afloat is down [Fig. 6 (a)], the spur line filter is connected to the circuit, and at the stub resonant frequency, there is an equivalent series open circuit that reflects the signal. However, when the afloat is up, the spur line filter is not connected to the circuit [Fig. 6 (b)]. Therefore, radiation occurs at all frequencies.
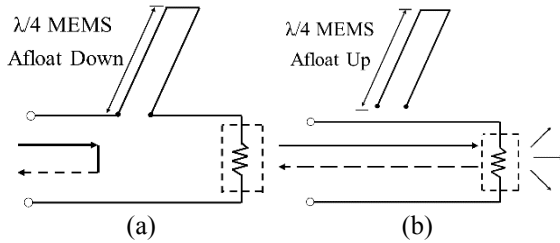
Fig. 6. Transmission line model for antenna with: (a) U-shaped afloat down, and (b) U-shaped afloat up.

IV. RESULTS AND DISCUSSION

In this paper, the MEMS mechanical structure is simulated using Intellisuite, which is a multi-physics simulator that uses the finite element method (FEM). For the mechanical simulations, it was assumed that aluminum afloat with a thickness of 5 µm is suspended 45 µm above the ground plane. Aluminum has a Young's modulus (E) of 70 GPa, a Poisson's ratio (v) of 0.33, and a density (ρ) of 2700 kg/m^3. Figure 7 shows the afloat displacement versus bias voltage from 0 V to 16 V. The deflection as a function of voltage increases slightly until a drastic change occurs that indicate pull in voltage. The pull-in voltage of the afloat is about 15.9 V, which is low comparing to previous designs, and the switching is permanent. This means that the switch has the ability to stay in down position constantly. The calculated pull-in voltage using Eq. 4 is 16.4 V. Hence, for considerably large structure of the afloat comparing to previous MEMS switches, there is good agreement between analatical and simulation result for afloat pull-in voltage.
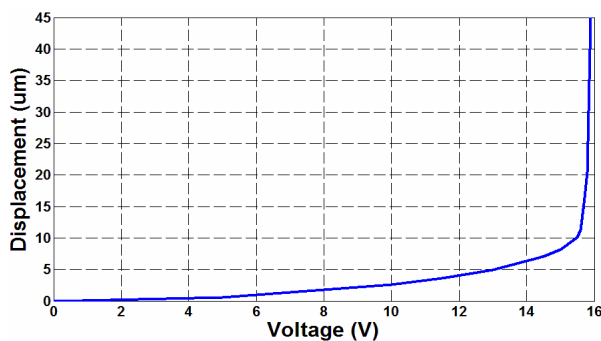

Fig. 7. Afloat displacement vs. DC voltage.

Figure 8 shows the simulated S_{11} results for the proposed antenna. When the afloat is up, the simulated plots for the antenna (afloat up) and the "Reference" antenna (the antenna presented in Fig. 1 without afloat) are in very good agreement. This agreement indicates the efficiency of the afloat has least effect on the antenna's performance. When the afloat is down, the presented reflection coefficient verifies the good performance of the MEMS afloat and the suggested effectiveness.

As shown in Fig. 9, the antenna's gain decreases sharply over 7 dB in the notched band. For other frequencies, out of the notched band, the antenna exhibits moderate gain about 3.2 dBi.

Figure 10 shows the simulated S_{11} characteristics for different values of D. As D increases from 0.82 to 1.82 mm, the bandwidth of notched band is varied from 560 to 410 MHz. From this result, the band width of notched band is controllable by changing of the slot. By decreasing of D, the slot gets closer to the edges and bottom of antenna so it can absorb waves easier in the wider ranges of frequency from center resonant frequency. It can be seen that by changing D, the center frequency of notched band remains almost fixed.
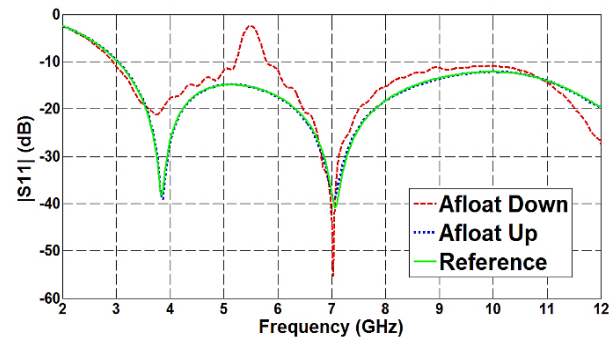

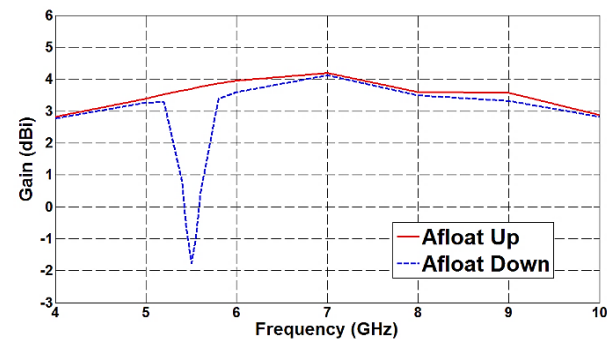Fig. 8. Simulated reflection coefficient of the antenna.

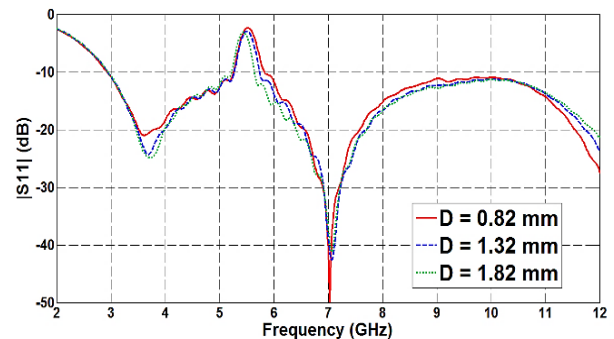Fig. 9. Simulated realized gain of the antenna.

Fig. 10. Slot position effect on reflection coefficient.

Figure 11 shows the simulated S_{11} characteristics for different values of L_N. As L_N increases from 7.1 to 8.7 mm, the center frequency of notched band is varied from 5.88 to 5.12 GHz. From this result, the frequency of notched band is controllable by changing length of the slot and it decreases 47.5 MHz for every 1 mm increase of L_N, which agrees with Eq. 10. It can be seen that by changing L_N, the bandwidth of notched band remains almost fixed.

Figure 12 shows the simulated S_{11} characteristics for different values of h. As the height h increases from 25 to 65 μm, the center frequency of notched band is varied from 5.43 to 5.63 GHz. From this result, the frequency of notched band increases 50 MHz for every 10 μm increase of h. By increasing the height of h the ε_{eff} decreases, and according to Eq. 10, the resonant frequency increases. It can be seen that the bandwidth of notched band remains almost fixed.
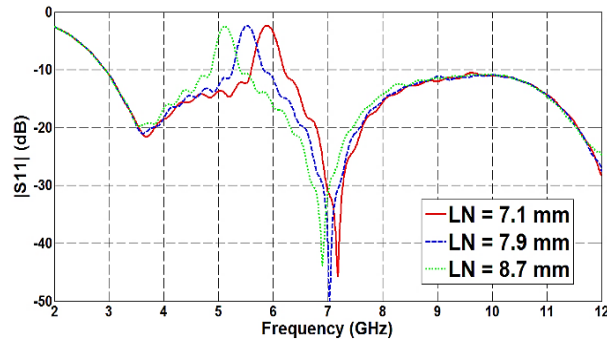
While the afloat is up, the variation of the group delay of the antenna is about 1 ns across the whole UWB. If the group delay variation exceeds 1 ns, the phases are no longer to be linear in far-field region and a pulse distortion is caused. It can be a serious problem in UWB communication systems. On the other hand, while the afloat is down, the maximum group delay of 6.5 ns happens in notched frequency. Figure 15 shows the group delay of the antenna, while the antennas are put side by side in a distance of 20 cm. While the afloat is up, the group delay of the antenna is about 1 ns across the whole UWB. On the other hand, while the afloat is down, the maximum group delay of 11.5 ns happens in notched frequency. This study has shown that band-notched antenna has a good time-domain characteristic and a small pulse distortion as well.

Fig. 13. The setup of the group delay simulation.

Fig. 11. Slot length effect on reflection coefficient.

Fig. 14. Simulated group delay of the antenna in face to face position.
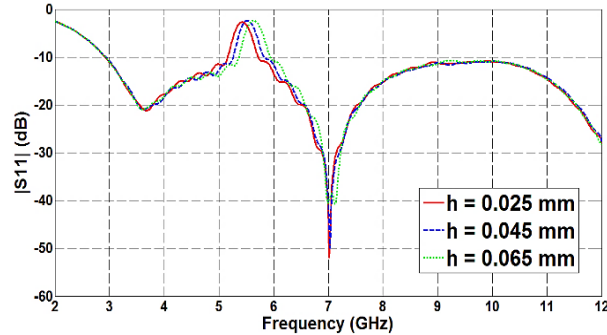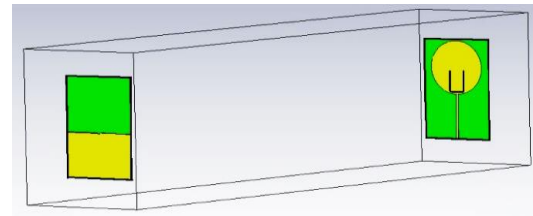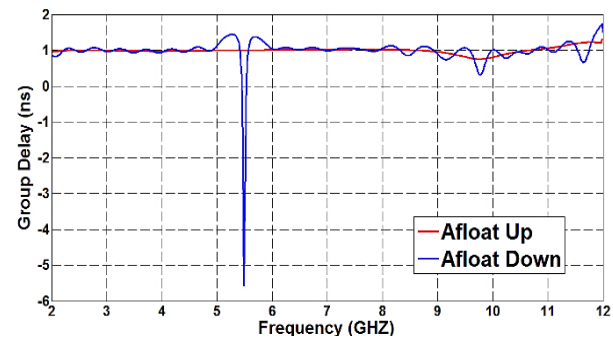

Fig. 12. Slot height effect on reflection coefficient.

Although, the proposed antenna presents very wide frequency band, the good frequency domain performance cannot necessarily ensure that the antenna also behaves well in time-domain. As a result, in order to verify the effectiveness of the antenna for time-domain applications, its time-domain response must be examined. The time-domain characteristic of the antenna is simulated in a manner shown in Fig. 13. The two identical proposed antennas are put face to face in a distance of 20 cm. The simulated group delay of the antenna is shown in Fig. 14.
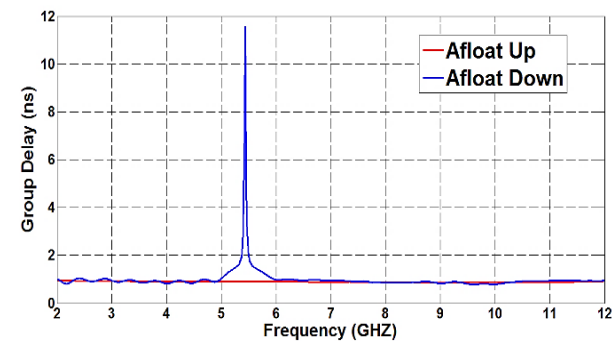

Fig. 15. Simulated group delay of the antenna in side by side position.

Figure 16 and 17 shows the radiation patterns for the antenna. Simulations at 5.5 and 8 GHz are presented in both E (x-y) and H (x-z) planes. The two states (afloat up and down) of the reconfigurable antenna are compared with the "Reference" antenna. Radiation patterns at 8 GHz show that the addition of the resonating elements does not affect the radiation performance of the antenna,
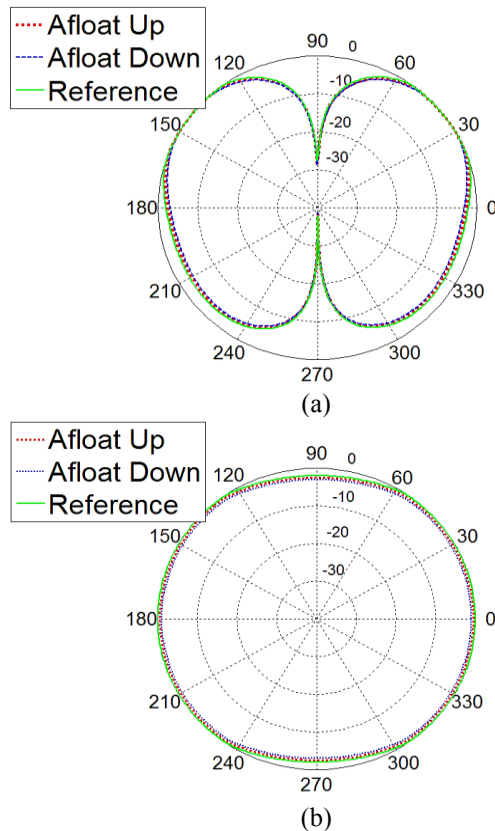
outside the of the notch band frequencies [Figs. 16 (a) and (b)]. On the other hand, within the band-notch range (radiation patterns at 5.5 GHz) and with the appropriate MEMS afloat state the radiated field intensity is degraded [Figs. 17 (a) and (b)]. It can be seen from Figs. 16 and 17 that, the presence of the afloat has least effect on the radiation patterns except when it goes down.
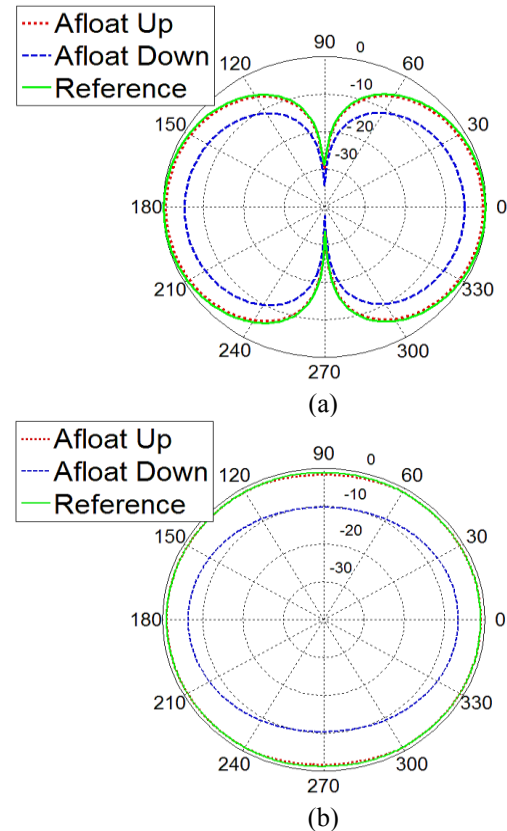

Fig. 16. Simulated radiation pattern at: (a) E plane at 8 GHz and (b) H plane at 8 GHz.

Fig. 17. Simulated radiation pattern at: (a) E plane at 5.5 GHz and (b) H plane at 5.5 GHz.

VI. CONCLUSION

An ultra wideband (UWB) elliptical monopole antenna fed by microstrip line with reconfigurable rejection band characteristic at the WLAN band (5.15-5.825 GHz) is proposed in this paper. To obtain reconfigurability, a $\lambda/2$ long U-shaped MEMS afloat is used, which is actuated through the RF signal path without DC bias lines. Using extra DC bias lines could reduce the radiation performance of the antenna because of RF leakage through the bias lines. The effects of the various geometrical parameters on the notched frequency band are studied. The pull in voltage of the afloat was low and its switching was permanent. Due to a novel afloat design, the proposed antenna has good omnidirectional pattern in different frequencies and the addition of the resonance element does not affect on the radiation performance outside of notched band frequencies.

REFERENCES

[1] Federal Communications Commission Re-vision of Part 15 of the Commission's Rules Regarding Ultra-wideband Transmission System" Tech. Rep., ET-Docket 98-153, FCC02-48, 2002.

[2] R. Chair, A. A. Kishk, K. F. Lee, C. E. Smith, and D. Kajfez, "Microstrip line and CPW fed ultra-wideband slot antennas with U-shaped tuning stub and reflector," *Progress In Electromagnetics Research*, vol. 56, pp. 163-182, 2006.

[3] D. Chen and C. H. Cheng, "A novel compact ultra-wideband (UWB) wide slot antenna with via holes," *Progress In Electromagnetics Research*, vol. 94, pp. 343-349, 2009.

[4] K. P. Ray and Y. Rang, "Ultra wideband printed elliptical monopole antennas," *IEEE Transactions on Antennas and Propagation*, vol. 55, no. 4, pp.

1189-1192, 2007.

[5] N. Ojaroudi, M. Ojaroudi, and Sh. Amiri, "Enhanced bandwidth of small square monopole antenna by using inverted U-shaped slot and conductor-backed plane," *Applied Computational Electromagnetics Society (ACES) Journal*, vol. 27, no. 8, pp. 685-690, Aug. 2012.

[6] R. Fallahi, A.-A. Kalteh, and M. Golparvar Roozbahani, "A novel UWB elliptical slot antenna with band-notched characteristics," *Progress In Electromagnetics Research*, vol. 82, pp. 127-136, 2008.

[7] Y. J. Cho, K. H. Kim, D. H. Choi, S. S. Lee, and S-O. Park, "A miniature UWB planar monopole antenna with 5-GHz band-rejection filter and the time-domain characteristics," *IEEE Trans Antennas Propag.*, vol. 54, no. 5, pp. 1453-1460, 2006.

[8] T. P. Vuong, A. Ghiotto, Y. Duroc, and S. Tedjini, "Design and characteristics of a small U-slotted planar antenna for IR-UWB," *Microwave Opt. Technol. Letters*, vol. 49, iss. 7, pp. 1727-1731, 2007.

[9] M. Majidzadeh and C. Ghobadi, "Compact microstrip fed monopole antenna with modified slot ground plane for UWB applications," *Applied Computational Electromagnetics Society (ACES) Journal*, vol. 27, no. 10, pp. 801-807, Oct. 2012.

[10] S. Khan, J. Xiong, and S. He, "Low profile and small size frequency notched planar monopole antenna from 3.5 to 23.64 GHz," *Microwave Opt. Technol. Letters*, vol. 50, iss. 1, pp. 235-236, Jan. 2008.

[11] R. Zaker, C. Ghobadi, and J. Nourinia, "Novel modified UWB planar monopole antenna with variable frequency band-notched function," *IEEE Antennas Wireless Propag. Letters*, vol. 7, pp. 112-114, 2008.

[12] W. Chen and K. Yang, "CPW-fed planar ultra-wideband antenna having a frequency band-rejected function," *Proc. Int. Conf. TENCON2007*, pp. 1-3, 2007.

[13] Y. Li, W. Li, and W. Yu, "A switchable UWB slot antenna using SIS-HSIR and SIS-SIR for multi-mode wireless communications applications," *Applied Computational Electromagnetics Society (ACES) Journal*, vol. 27, no. 4, pp. 340-351, Apr. 2012.

[14] V. A. Shameena, M. N. Suma, K. Raj Rohith, P. C. Bybi, and P. Mohanan, "Compact ultra-wideband planar serrated antenna with notch band ON=OFF control," *Electron. Lett.*, vol. 42, no. 23, pp. 1323-

1324, Nov. 2006.

[15] S. Nikolaou, N. D. Kingsley, G. E. Ponchak, J. Papapolymerou, and M. Tentzeris, "UWB elliptical monopoles with a reconfigurable band notch using MEMS switches actuated without bias lines," *IEEE Trans. Antennas Propag.*, vol. 57, no. 8, pp. 2242-2251, 2009.

[16] D.-M. Fang, S. Fu, Y. C. Yong, and X.-L. Zhao, "Surface micromachined RF MEMS variable capacitor," *Microelectronics Journal*, vol. 38, no. 8-9, pp. 855-859, 2007.

[17] W.-S. Lee, D.-Z. Kim, K.-J. Kim, and J. W. Yu, "Wideband planar monopole antennas with dual band-notched characteristics," *IEEE Trans. Microw. Theory Tech.*, vol. 54, no. 6, pp. 2800-2806, Jun. 2006.

Arash Nemati was born in Ghaemshahr, Iran, in 1989. He received the B.S. degree in Electrical Engineering from University of Mazandaran, Babolsar, Iran, in 2011 and M.S. degree in Electronics from Babol University of Technology, Babol, Iran, in 2014.

Since February 2014, he has been a Lecturer at the Department of Electrical and Computer Engineering, Babol University of Technology, Babol, Iran. His research interests include RF Microelectronics, RF-MEMS, Reconfigurable Antennas and Filters, and CMOS Analog Integrated Circuit Design.

Bahram Azizollah Ganji is an Associate Professor of Micro-Electronics with the Babol Noshirvani University of Technology. He received his Ph.D. degree in Micro-Engineering and Nano-Electronics from the University Kabangsaan Malaysia (UKM) in 2007, his B.Sc. degree in Electronics from Mashhad University in 1987, and his M.Sc. degree in Electronics from Tehran University in 1983.

His current interests are design and fabrication of MEMS/NEMS sensors, RFMEMS, BiOMEMS, MOEMS and Nano-Electronics. He has published more than 70 academic research papers.